Fibrinogen-specific antibody induces abdominal aortic aneurysm in mice through complement lectin pathway activation

Hui-fang Zhou[a,1], Huimin Yan[a,1], Paula Bertram[a], Ying Hu[a], Luke E. Springer[a], Robert W. Thompson[b], John A. Curci[b], Dennis E. Hourcade[a], and Christine T. N. Pham[a,2]

[a]Division of Rheumatology, Department of Medicine, and [b]Division of Vascular Surgery, Department of Surgery, Washington University in St. Louis, St. Louis, MO 63124

Edited by K. Frank Austen, Brigham and Women's Hospital, Boston, MA, and approved October 8, 2013 (received for review August 15, 2013)

Abdominal aortic aneurysm (AAA) is a common vascular disease associated with high mortality rate due to progressive enlargement and eventual rupture. There is currently no established therapy known to alter the rate of aneurysmal expansion. Thus, understanding the processes that initiate and sustain aneurysmal growth is pivotal for the development of medical therapies aimed at halting disease progression. Using an elastase-induced AAA mouse model that recapitulates key features of human AAA, we previously reported that a natural IgG antibody directs alternative pathway complement activation and initiates the inflammatory process that culminates in aneurysmal development. The target of this natural antibody, however, was unknown. Herein we identify a natural IgG that binds to fibrinogen deposited in elastase-perfused aortic tissues, activates the complement lectin pathway (LP), and induces AAA. Moreover, we establish that alterations in the glycosylation patterns of this antibody critically affect its ability to activate the LP in vivo. We find that LP activation precedes the alternative pathway and absence of the LP complement protein mannan-binding lectin abrogates elastase-induced AAA. In human AAA tissues the mouse anti-fibrinogen antibody recognizes epitopes that localize to the same areas that stain positively for mannan-binding lectin, which suggests that the complement LP is engaged in humans as well. Lastly, we demonstrate that circulating antibodies in a subset of AAA patients react against fibrinogen or fibrinogen-associated epitopes in human aneurysmal tissues. Our findings support the concept that an autoimmune process directed at aortic wall self-antigens may play a central role in the immunopathogenesis of AAA.

Abdominal aortic aneurysm (AAA) is a common vascular disorder that affects ~5% of men and ~1.5% of women ages 65 and older (1, 2). Rupture of AAA presents a medical emergency that accounts for 15,000 deaths annually in the United States (3). Currently, surgical repair represents the only treatment option for large AAAs, whereas surgery in small AAAs offers no clear overall long-term survival advantage (4, 5). Thus, medical management, to inhibit or reverse the progression of small AAAs, has received increasing attention. Major challenges remain in the development of therapeutic agents that impede aneurysm expansion, as our understanding of the pathophysiology underlying this disease is incomplete.

One of the defining characteristics of AAA is inflammation accompanied by a cellular infiltrate that is predominantly lymphocytic (6–8). The elastase-induced AAA mouse model recapitulates many key features of human AAA, including the inflammatory response (9). We previously established with this model that aneurysm development requires factor B and properdin of the complement alternative pathway (AP) (10, 11). We showed that mice deficient in B cells (and hence antibodies), called μMT mice, are protected against aneurysm formation. Reconstitution with natural IgG, but not IgM, from wild-type mice restores susceptibility to the elastase-induced AAA phenotype (11). These results suggest that mouse IgG recognizes a self-antigen that is revealed following elastase perfusion and the antibody–antigen complex activates complement in the initiation of the inflammatory cascade (10, 11). Congruent with our findings in the animal model, previous studies of human AAA tissues revealed the presence of B cells and IgG antibodies sometimes seen in organized follicle-like structures, raising the question that AAA is the result of a dysregulated autoimmune response against putative aortic wall self-antigens (7, 12–15). However, the identity of a pathogenic autoantigen/autoantibody in AAA remains elusive. We report herein the identification of a natural anti-fibrinogen IgG antibody that induces the AAA phenotype in μMT mice through complement lectin pathway (LP) activation.

Results

Natural Mouse IgG Antibodies Recognize Extracellular Matrix Proteins in the Elastase-Perfused Aorta. A key step in aneurysmal development in the mouse model occurs when pathogenic natural IgG antibodies bind to antigens exposed or unmasked by elastase perfusion and form immune complexes (ICs) that mediate complement activation (11). To capture these ICs, we perfused WT mice with elastase, then harvested the aortas immediately after perfusion (T0) or at 30 min (T30). The aortic lysates from homogenized samples were cleared and incubated with protein

Significance

Abdominal aortic aneurysm (AAA) is a common and potentially fatal vascular disease. Although surgery is recommended for large aneurysms, surgical repair offers no clear survival advantage for small AAAs. A deeper understanding of the mechanisms that underlie disease pathogenesis could suggest strategies for medical intervention. Herein we identify a natural mouse IgG antibody that recognizes fibrinogen deposited in human AAA tissues and induces aneurysm in a mouse model through activation of the complement lectin pathway (LP). Conversely, absence of antibody or complement proteins abrogates AAA development. These results support the concept that antibody directed against aortic wall epitopes initiates LP activation that culminates in AAA formation. The antibody response and complement LP may provide therapeutic targets for halting disease progression.

Author contributions: H.-f.Z., H.Y., P.B., D.E.H., and C.T.N.P. designed research; H.-f.Z., H.Y., P.B., Y.H., and L.E.S. performed research; R.W.T., J.A.C., and D.E.H. contributed new reagents/analytic tools; H.-f.Z., H.Y., Y.H., L.E.S., and C.T.N.P. analyzed data; and H.-f.Z., H.Y., P.B., D.E.H., and C.T.N.P. wrote the paper.

The authors declare no conflict of interest.

This article is a PNAS Direct Submission.

[1]H.-f.Z. and H.Y. contributed equally to this work.

[2]To whom correspondence should be addressed. E-mail: cpham@dom.wustl.edu.

This article contains supporting information online at www.pnas.org/lookup/suppl/doi:10.1073/pnas.1315512110/-/DCSupplemental.

G-Sepharose beads to capture ICs formed following elastase perfusion. Protein samples were eluted from the beads and fractionated by SDS/PAGE. Protein bands of ~50 kDa and ~66 kDa apparent molecular weight were observed in comparable amounts in both the T0 and T30-min samples (Fig. 1*A*) and deemed likely to represent IgG heavy chain and albumin, respectively. Also present were bands of ~80 kDa and >250 kDa that appeared de novo at T30 and bands of ~130 kDa and ~250 kDa that were more prominent at T30 than T0. These bands were excised from the gel and identified by mass spectroscopy (MS) as type I collagen and fibrinogen (Fig. 1*B*).

Type I collagen is a major structural component of the aortic wall and consists of heterotrimeric polypeptide α-chains (16). The collagen α-chains identified were immunoprecipitated as monomers (130 and 138 kDa) as well as covalently cross-linked oligomers of ~250 and ~400 kDa. Fibrinogen is a heteromultimeric protein composed of three different chains (α, β, and γ) and plays an essential role in coagulation during which it is cleaved by thrombin to generate fibrin (17). The fibrinogen γ-chain (49 kDa) that was immunoprecipitated migrated as an ~80 kDa entity, suggesting that it may represent covalently cross-linked γ-chain dimers that are generated in the conversion of soft clots to hard clots (18). Previous studies showing that polyclonal rabbit antibodies directed against fibrinogen react with matrix proteins in human aneurysmal tissues (13), combined with a report that IgG isolated from human AAA specimens recognize an 80 kDa band in aneurysmal extracts (14), prompted us to further investigate fibrinogen as a candidate self-antigen in elastase-induced AAA.

A Natural IgG That Recognizes Fibrinogen Induces the AAA Phenotype. To obtain a natural IgG antibody that recognizes fibrinogen, fibrinogen cross-linked, or degradation products we fused splenocytes and lymphocytes from unmanipulated WT C57BL/6 mice with the myeloma cell line Sp20 and screened hybridoma clones for reactivity against purified mouse fibrinogen. We identified two clones, named C9 and G10, which produced monoclonal antibody (mAb) that reacted specifically with fibrinogen on Western blot analysis (Fig. 2 *A* and *B*). These mAbs, both IgG2b, κ, likely recognize peptide sequences common to the different fibrinogen chains, which is the typical polyreactivity pattern of natural antibodies. In addition, C9 and G10 mAbs cross-reacted with the α-chain of human fibrinogen (Fig. 2*B*) but not types I and III mouse collagen (Fig. 2*A*).

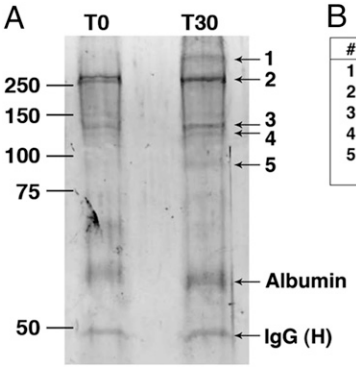

B

#	Protein ID	M.W. (kDa)
1	Collagen α2 (I)	130
2	Collagen α2 (I)	130
3	Collagen α1 (I)	138
4	Collagen α2 (I)	130
5	Fibrinogen γ	49

Fig. 1. Identification of aortic wall self-antigens. Groups of mice were perfused with elastase, then killed immediately (T0, $n = 3$) or after 30 min (T30, $n = 3$). Preformed ICs were immunoprecipitated as detailed in *Materials and Methods* and analyzed by SDS/PAGE under reducing conditions. (*A*) Bands that were enhanced or appeared de novo (nos.1–5) were excised and submitted for MS analysis. (*B*) Identity (ID) and molecular weight (MW) of protein bands identified by MS.

We have previously established that transfer of purified mouse natural IgG antibody restored aneurysm susceptibility to the normally resistant μMT mice in the elastase-induced model of AAA (11). To evaluate the pathogenic potential of the C9 and G10 mAbs, we used the same elastase-induced model of AAA, in which transient perfusion of the abdominal aorta with a dilute porcine elastase solution on day 0 consistently leads to antibody-dependent aneurysm formation by day 14 (10, 11, 19). Immediately after elastase perfusion, we transferred 250 μg of purified C9, G10, or IgG2b, κ-isotype control i.v. into μMT mice, which were previously shown to be resistant to AAA (11). Both C9 and G10 mAbs reacted equally with aortic wall tissues of elastase-perfused μMT mice but not nonperfused aortas (Fig. 2 *C* and *D*). Next we tested their ability to induce AAA in μMT mice. In this model, aneurysm development is defined as an increase in aortic diameter (AD) of greater than 100% over the preperfused diameter (10, 11, 19). Unexpectedly, we found that G10 mAb transfer led to AAA development, whereas C9 mAb transfer did not (Fig. 3*A*). Aneurysm development in G10-treated μMT mice was accompanied by fragmentation of elastic fibers (Fig. 3*B*) and depletion of smooth muscle cell (SMC) actin (Fig. 3*C*), characteristics of the AAA disease phenotype in WT animals as previously established (10, 11, 19). In contrast, we observed in C9-treated μMT mice relatively preserved elastic fibers (Fig. 3*D*) and SMC actin content (Fig. 3*C*), similar to untreated μMT mice or μMT mice treated with the isotype control. These results establish that the anti-fibrinogen G10 mAb is pathogenic in the elastase-induced AAA model.

G10 mAb Binds Mannan-Binding Lectin and Initiates the Complement Cascade. Pathogenicity of G10 mAb required the fragment crystallizable (Fc) portion of the IgG, as treatment of μMT animals with the G10 $F(ab')_2$ fragment that lacks the Fc region did not reconstitute the AAA phenotype (Fig. 3*A*). This led us to reason that the differential capacity of G10 and C9 mAbs to induce AAA might be caused by structural variations in the Fc portion of the IgG. Although the primary amino acid sequence is conserved within the Fc region of the IgG2b subclass, there is considerable heterogeneity in the sugar residues attached to asparagine 297 (Asn^{297}) within the heavy chain domain CH2 of each IgG Fc portion (20). The Asn^{297}-linked glycan contains a biantennary carbohydrate structure that is characterized by the absence or presence of terminal galactose residues: IgG(G0) has no galactose; IgG(G1) has galactose on one arm; and IgG(G2) has galactose on both arms (21, 22) (Fig. 4*A*). To investigate whether C9 and G10 mAbs harbor different Asn^{297}-linked glycoforms, we subjected each to blotting with *Erythrina cristagalli* lectin (ECL), a legume lectin that binds terminal galactose residues (23). ECL bound readily to C9 mAb but poorly to G10 mAb, suggesting reduced terminal galactosylation in G10 mAb (Fig. 4*B*).

Malhotra et al. showed that the absence of terminal galactose residues exposes the *N*-acetyl glucosamine (GLcNAc) in the IgG core glycan that binds mannan-binding lectin (MBL) and initiates complement activation (24). To determine whether G10 mAb activates the LP, we first we tested its ability to bind mouse MBL, a pattern-recognition molecule that directs LP activation. Monoclonal antibodies immobilized to microtiter wells were subjected to several dilutions of mouse serum to test their ability to capture MBL. The results indicated that G10 mAb binds more readily to the MBL form MBL-C than does C9 mAb (Fig. 4*C*). We next asked whether G10 mAb activates the LP in vivo. To this end, μMT mice were perfused with elastase followed immediately by an i.v. dose (250 μg) of mAb or isotype control. Immunofluorescence performed on aortic sections isolated 30 min after perfusion showed that G10 colocalized with MBL-C in the aortic wall (Fig. 4*D*). In contrast, there was no deposition of the recognition subcomponent C1q of the classical pathway (CP)

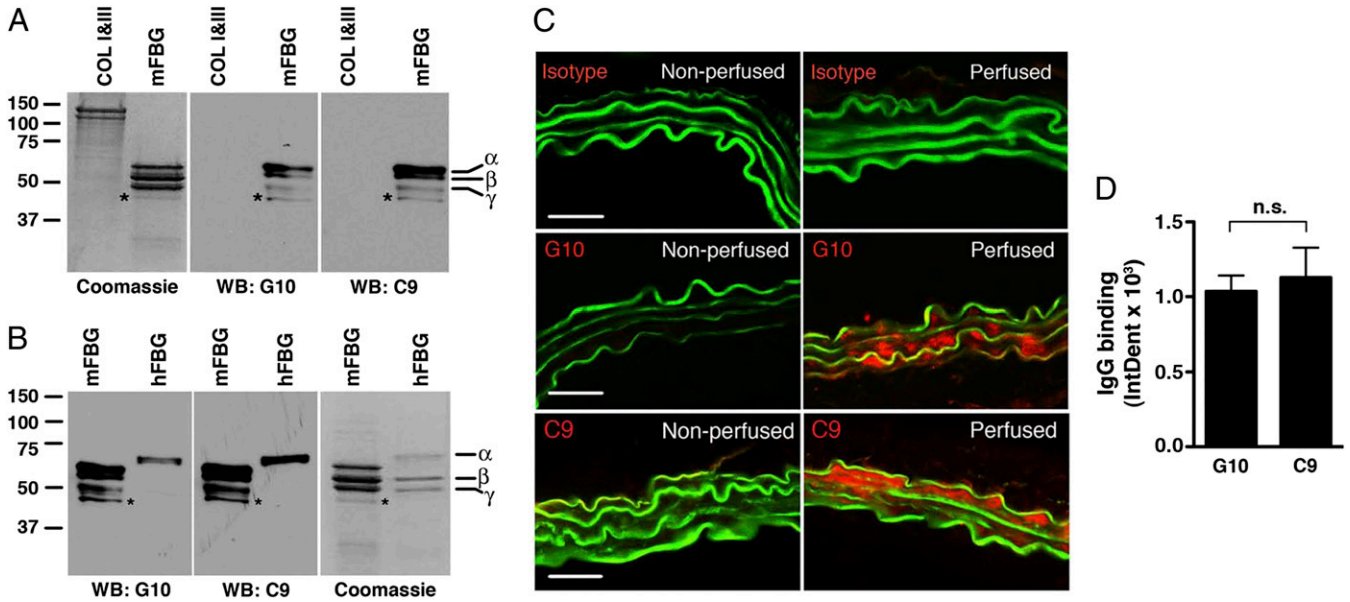

Fig. 2. Cloning of anti-fibrinogen antibodies. Screening of hybridoma clones using mouse fibrinogen as an antigen identified two mAbs, G10 and C9, that recognize different chains of mouse fibrinogen (mFBG) (*A*) and human fibrinogen (hFBG) (*B*) but not mouse types I and III collagen (COL), as determined by Western blot (WB) analysis. *Minor band that likely represents degradation product of one of the major chains. Coomassie-blue stained gel served as protein loading control. (*C*) G10 and C9 mAbs bind to elastase-perfused aortic wall. μMT mice were left nonperfused (negative control) or perfused with elastase followed by i.v. transfer of 250 μg of IgG isotype control or the indicated mAb. Thirty minutes after perfusion, aortas were harvested and bound mAbs were detected with an anti-mouse IgG (red). The elastic fibers are autofluorescent (green). Representative photomicrographs are shown. (Scale bar, 50 μm.) (*D*) Quantitative analysis of G10 and C9 binding to abdominal aortas 30 min after elastase perfusion and mAb transfer. $n = 3$ aortas per treatment, six to nine sections per aorta. The mean integrated OD (IntDen) ± SEM per aortic cross-section was calculated as detailed in *Materials and Methods*. NS, not significant.

detected in perfused aortas (Fig. S1), which explains the lack of CP involvement in this model (10, 11). G10 mAb activates the complement cascade, as evidenced by abundant MBL-C and C3 deposition (Fig. 4 *E* and *F*). In contrast C9 mAb transfer only led to minimal MBL-C and C3 deposition (Fig. 4 *E* and *F*). Taken together the results suggest that the pathogenic capacity of the G10 mAb was due to the recognition of the G10 IgG(G0) glycoforms by MBL that facilitated a robust LP-dependent complement activation cascade necessary for the ensuing aneurysmal phenotype.

Agalactosylated C9 mAb Is Pathogenic. If the in vivo pathogenicity of G10 could indeed be attributed to reduced terminal galactosylation at the Asn^{297} site, then we reasoned that C9 mAb could be made pathogenic by removing its terminal Asn^{297}-linked galactose residues. To that end, C9 mAb was treated with β-galactosidase and reduction in terminal galactosylation was evaluated and confirmed by ECL blotting (Fig. 5*A*). Moreover, galactose-depleted C9 mAb bound MBL-C in vitro at ∼1.5-fold better than did untreated C9 mAb (Fig. 5*B*). Lastly, agalactosylated C9 mAb directed robust LP activation in the elastase-perfused aortic wall (Fig. 5 *C* and *D*) and induced aneurysm in μMT mice (Fig. 5*E*). These results further demonstrate the regulatory role that the Asn^{297}-linked glycoforms play in autoantibody activity and pathogenicity in elastase-induced AAA.

The LP Is Activated Upstream of the AP in Elastase-Induced AAA. We have previously shown that natural antibodies and the AP are essential for aneurysm development, whereas the CP is dispensable (10, 11). Although the evidence available at that time did not rule out a role for the LP, we offered a model in which antibodies may directly initiate the AP. The most recent evidence obtained herein, however, supports a sequence of events in which the LP is directly activated by antibody–MBL interactions and that the LP subsequently engages the AP feedback loop. In view of this model, we evaluated the contribution of the LP in the AAA model. The human LP is composed of five different carbohydrate recognition subcomponents: MBL, three ficolins (L-ficolin, H-ficolin, and M-ficolin), and collectin 11 (CL-11). In the mouse, there are two forms of MBL, MBL-A and MBL-C. We found that mice deficient in MBL-A and MBL-C (MBL-A/$C^{-/-}$) were indeed resistant to elastase-induced AAA (Fig. 6*A*). This result demonstrates that LP dependence is not restricted to the special case wherein disease is induced in μMT mice by the G10 mAb but also extends to the general case in which a full repertoire of natural antibodies is present. It also confirms our previous conclusion that the CP does not play an important role in the mouse because it does not substitute for the LP. We further determined that antibody recognition of aortic wall self-antigens preceded and was independent of MBL, as we found abundant IgG deposition in elastase-perfused MBL-A/$C^{-/-}$ aorta (Fig. 6*B*). To further dissect whether AP activation occurs in the context or independent of LP activation, we looked for deposition of properdin, an AP protein. We found that properdin is abundantly deposited in elastase-perfused WT but not MBL-A/$C^{-/-}$ aorta (Fig. 6 *B* and *C*). Absence of staining in WT aorta with an isotype control confirmed the specificity of the properdin antibody (Fig. 6*B*). Taken together, these results support the concept that AP activation occurs downstream of the LP. Thus, in this sequence of events, self-antigens exposed in elastase-perfused aorta are recognized by anti-fibrinogen antibody. The immune complex binds MBL, initiating LP activation that is subsequently amplified by the AP (Fig. 6*D*).

The LP Is Engaged in Human AAA. Multiple studies have implicated the complement cascade in the pathogenesis of human AAA (10, 25, 26). Evidence so far implicates both CP and AP; however, the role of the LP has not been explored. We examined human AAA tissues for evidence of LP activation and found abundant deposition of MBL throughout the aortic wall (Fig. 7). Particularly,

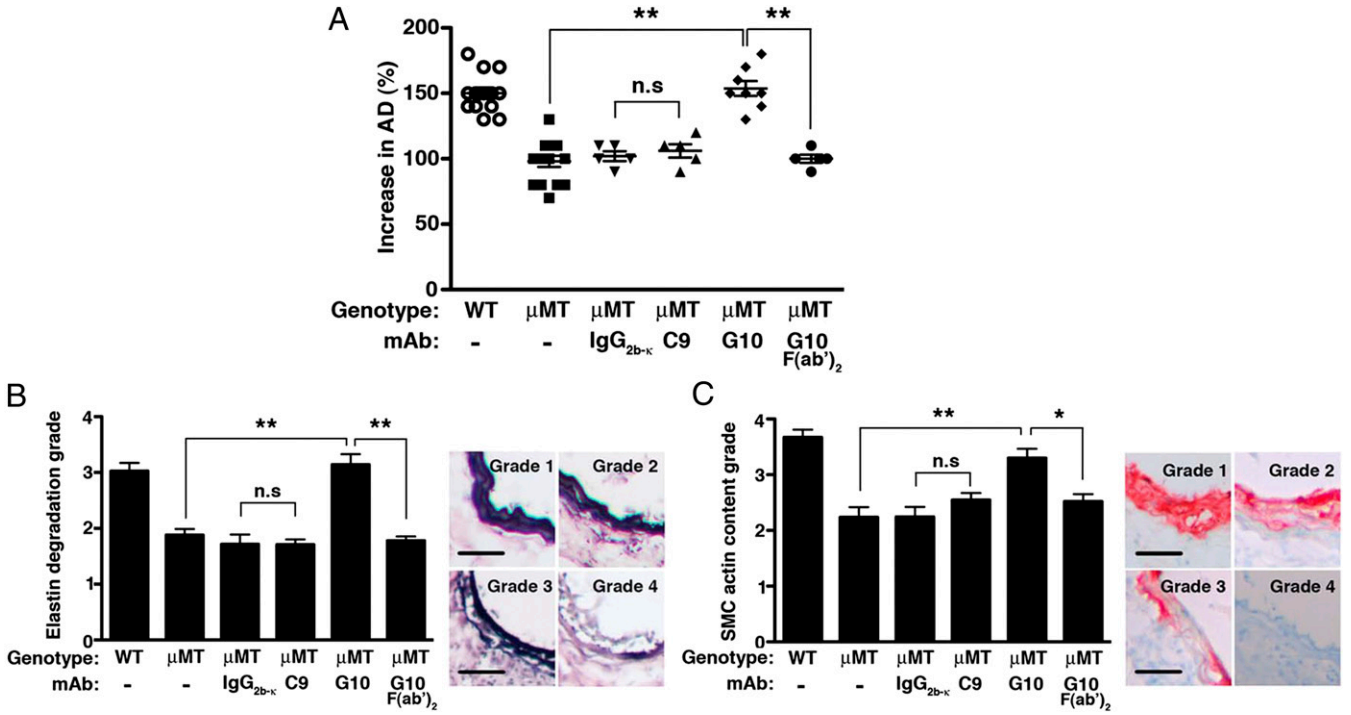

Fig. 3. Pathogenicity of anti-fibrinogen antibodies. (*A*) Mice were perfused on day 0 with elastase and randomly selected to receive an i.v. dose of 250 µg of the indicated mAb or isoptype control. On day 14 following elastase perfusion, the aortic diameter (AD) was reassessed and increase in AD was expressed in percentage (%). AAA is defined as an increase in AD of >100% over the preperfused diameter. Values represent mean ± SEM; each symbol represents an individual mouse. Day 14 elastic fiber degradation (*B*) and SMC actin content (*C*) were graded on a scale of 1–4 according to the keys shown on the *Right* and detailed in *Materials and Methods*. Values represent mean ± SEM, $n = 5$ aortas per genotype per treatment, six to nine slides per aorta. (Scale bar, 40 µm.) $^{*}P < 0.05$, $^{**}P < 0.001$, NS, not significant.

MBL was found in close association with infiltrating inflammatory cells (i.e., $CD68^{+}$ macrophages) (Fig. S2). Furthermore, we used the G10 mAb that cross-reacts with human fibrinogen α-chain (Fig. 2*B*) to probe AAA tissues and found that G10 mAb localized to the same areas in the aortic wall that stained positively for MBL (Fig. 7). Absence of staining with a mouse IgG isotype control confirmed that G10 mAb reacted specifically against fibrinogen and/or fibrinogen-associated epitopes in AAA tissue (Fig. S3*A*). Together, these results raise the possibility that an immune response against fibrinogen deposited in the aortic wall leads to the activation of the complement cascade in human AAA.

Anti-Fibrinogen Antibodies Are Present in the Circulation of Individuals with AAA. Although polyclonal rabbit anti-human fibrinogen antibodies have been shown to react with matrix fibrils in aneurysmal specimens (13), a circulating autoantibody in AAA patients with specificity against fibrinogen has not been described. We examined sera from AAA and non-AAA patients and found various levels of reactivity against fibrinogen in several AAA sera tested (Fig. 8*A*). Antibodies in reactive AAA sera bound to epitopes on different fibrinogen chains. Moreover, sera from AAA patients (Pt 3 and Pt 7) reacted against human aneurysmal tissues with a pattern similar to G10 reactivity (fibrinogen) (Fig. 8*B*). Preadsorption against human fibrinogen eliminated most of the specific staining (Fig. 8*C* and Fig. S3 *B* and *C*), which suggests that in these patients, antibody recognition of aneurysmal tissues was mediated predominantly by exposed fibrinogen and/or fibrin (ogen)-associated epitopes.

Discussion

We have investigated AAA development in a mouse disease model and report herein the identification of a natural anti-fibrinogen IgG antibody that induces AAA. These results, however, do not exclude the possibility that other natural antibodies may be able to bind additional aortic wall antigens that are unmasked by elastase perfusion. In addition, our analysis of human serum samples suggests that, in a subset of AAA patients, anti-fibrinogen antibodies mediate specific recognition of aneurysmal tissue epitopes. The presence of circulating anti-fibrinogen antibodies that recognize specific epitopes in human aneurysmal tissues increases the relevance of the experimental findings and lends further support to the hypothesis that AAA is an immune-mediated disease. In human AAA, although an association between fibrinogen, fibrin degradation products (i.e., D-dimer), and aneurysm size/progression has long been recognized (27, 28), a causal relationship has not been clearly established. The massive deposition of fibrin/fibrinogen and/or fibrin degradation products in human AAA tissue (26) is reminiscent of the increased local accumulation of fibrin/fibrinogen in the inflamed joints of individuals with rheumatoid arthritis (RA) (29), a disease in which autoantibody response to fibrinogen, specifically citrulline-modified fibrinogen (a process whereby the arginine residues of fibrinogen are converted to citrulline), is not only diagnostic but is thought to contribute to disease pathogenesis (30). Whether circulating antibodies with fibrinogen specificity drive the pathogenesis of human AAA and/or serve as biomarkers for disease progression in this subset of AAA patients remains to be determined.

It has been shown that the relative ability of IgG to activate complement (31, 32) and mediate pathogenesis is inversely correlated with the degree of terminal galactosylation (at Asn^{297}) (33). Indeed, serum levels of the IgG(G0) variant are increased in several autoimmune disorders, such as RA, and appear to correlate with disease activity (34). The absence of terminal galactose residues exposes the high mannose core carbohydrate structure that becomes accessible to MBL (24). Our results indicate that

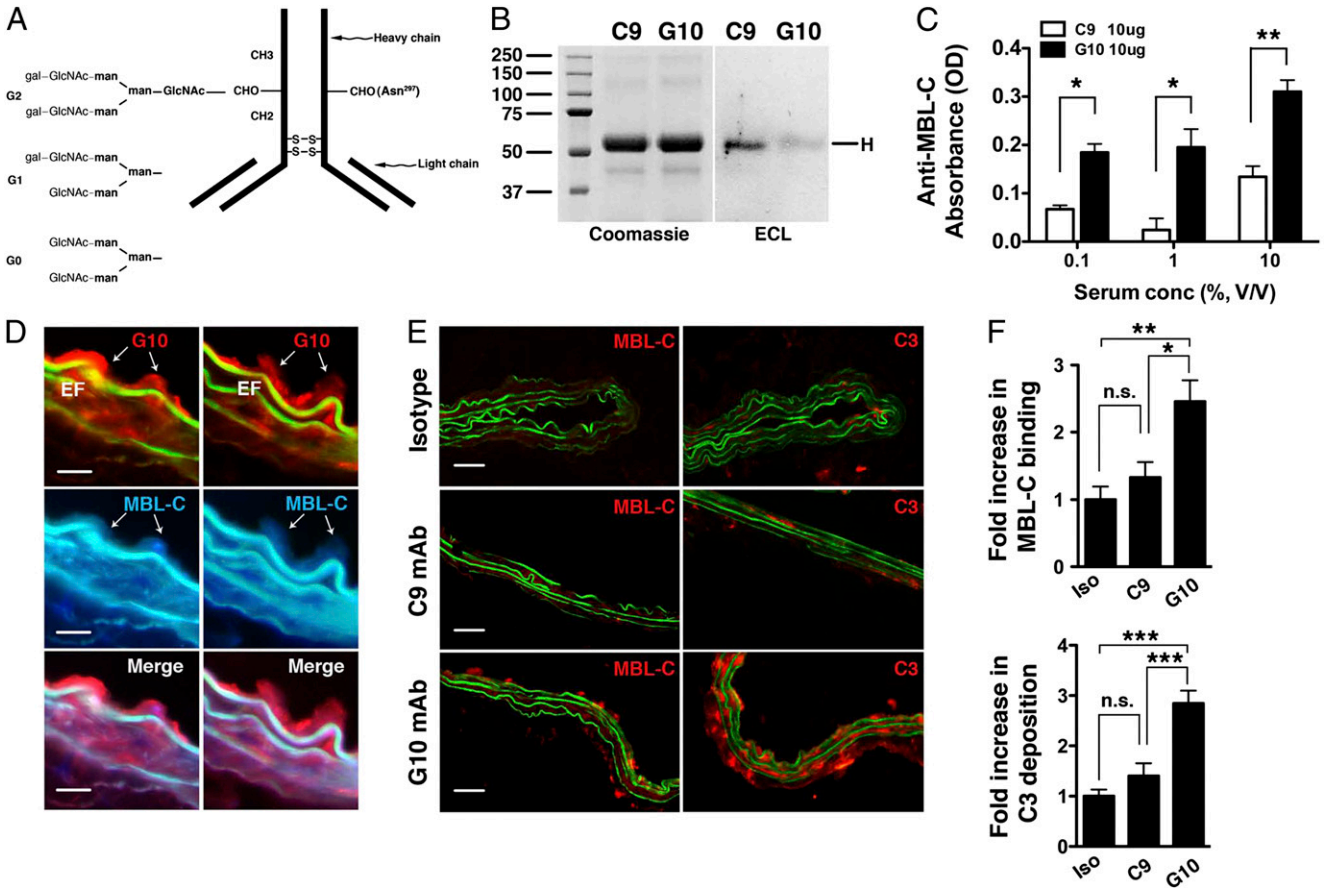

Fig. 4. Activity of anti-fibrinogen mAb glycovariants in complement activation. (*A*) Schematic depiction of different glycan chains linked to asparagine 297 (Asn^{297}) of the CH2 domain of IgG heavy chain. Gal, galactose; GLcNAc, *N*-acetyl glucosamine; man, mannose. (*B*) Blotting with *Erythrina cristagalli lectin* (ECL) detects the level of terminal galactosylation. Coomassie blue-stained gel is shown for protein loading control. (*C*) Mouse serum (as a source of MBL, at the indicated percentage of dilution) was incubated with plate-bound C9 or G10 mAb (10 μg/mL); MBL-C binding to the mAb was detected with an anti–MBL-C antibody. Data shown represent mean ± SEM of triplicate values derived from three independent experiments. $*P < 0.01$, $**P < 0.001$. (*D*) Aortas from elastase-perfused, G10-reconstituted μMT mice were probed for MBL-C (blue) and G10 (red) deposition. Representative sections showing colocalization of MBL-C and fibrinogen (detected with G10 mAb). Elastic fibers (EF) autofluoresce in green and blue spectra. (Scale bar, 15 μm.) (*E*) μMT mice were perfused with elastase and immediately injected with 250 μg of isotype control or the indicated mAb. Aortas were harvested at 30 min and examined for MBL-C (red) or C3 (red) deposition as evidence of complement activation. Representative photomicrographs are shown. (Scale bar, 50 μm.) (*F*) Quantitative analysis of MBL-C binding and C3 deposition in abdominal aortas 30 min after elastase perfusion and mAb transfer. $n = 3$ aortas per treatment, six to nine sections per aorta. Values represent fold increase in integrated OD (IntDen) ± SEM compared with isotype (iso) control (set at 1). $*P < 0.05$, $**P < 0.01$, $***P < 0.002$, NS, not significant.

G10 mAb harbors fewer terminal galactose residues than C9, as evidenced by lower ECL binding. As a result, G10 mAb binds more efficiently to MBL in vitro and activates the LP in vivo. Highly galactosylated C9 mAb, on the other hand, was unable to induce AAA until terminal galactose residues were removed, rendering the core glycan more accessible to MBL. Taken together, our results indicate that, regardless of antibody specificity, the glycosylation state of the IgG critically affects its interaction with and ability to activate the LP, underlining the importance of the IgG Fc-linked glycan structures in the development of elastase-induced AAA.

Finally, multiple lines of evidence indicate that the complement cascade likely participates in AAA pathogenesis. A recent study showed that C2, an essential component of both the CP and the LP, is abundantly deposited in AAA tissues (25). However, based on increased expression of C1q protein, the investigators concluded that the CP, not the LP, plays a more prominent role in human AAA. Here we show that MBL, an LP equivalent to C1q, is also present in human AAA tissues. The LP is increasingly recognized as an essential regulator of hemostasis/inflammation and a significant contributor to cardiovascular diseases (35–38). Inhibitors of the LP pathway modulate coagulation disorders and protect against ischemia/reperfusion injury (38, 39). The studies herein establish that antibody-mediated LP activation is essential in the pathogenesis of elastase-induced AAA. Although the role of antibody in complement AP activation/amplification has been studied (40, 41), and reports indicate that adherent immune complexes can induce AP activation in vivo (42, 43), direct antibody-mediated activation of the AP in elastase-induced AAA was not demonstrated (11). Instead, the results herein are consistent with our previous findings that properdin of the AP does not initiate C3 convertase assembly but serves mainly as a convertase stabilizer (11). It is now becoming apparent from this and other recent studies (44–47) that the LP triggers the initial complement activation and the AP serves to amplify the LP activity in many disease models. These results also suggest a more careful reexamination of the role of properdin and the AP in the pathogenesis of many disease processes (48) and the evaluation of properdin and other AP proteins as therapeutic targets. Thus, one could envision that inhibiting the AP alone may not alter the course of disease over time, as the unopposed LP activity continues to cause tissue injury, albeit at a slower pace

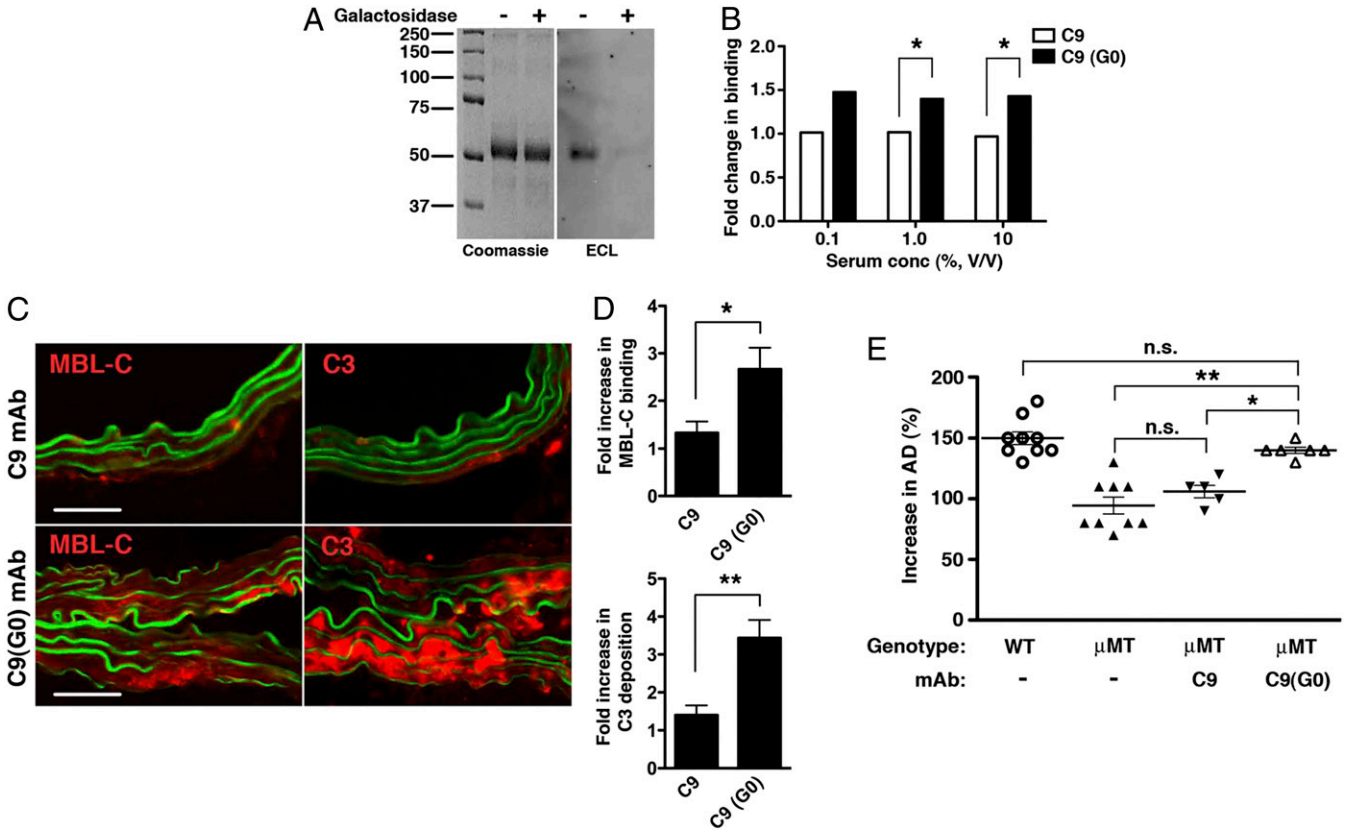

Fig. 5. Effect of galactose removal on C9 mAb activity. (*A*) Untreated and β-galactosidase–treated C9 mAbs were blotted with *Erythrina cristagalli* lectin (ECL) to confirm depletion of terminal galactose residues in C9(G0). Coomassie blue-stained gel is shown for loading control. (*B*) Binding of MBL-C to untreated C9 and galactose-depleted C9(G0) mAb. Data shown represent mean ± SEM of triplicate values derived from two independent experiments. $*P < 0.01$. (*C*) μMT mice were perfused with elastase and administered 250 μg of C9 or C9(G0) mAb i.v. At 30 min, aortas were harvested and examined for MBL-C (red) or C3 (red) deposition as evidence of complement activation. Representative photomicrographs are shown. (Scale bar, 50 μm.) (*D*) Quantitative analysis of MBL-C and C3 deposition in abdominal aortas 30 min after elastase perfusion and mAb transfer. $n = 3$ aortas per treatment, six to nine sections per aorta. Values represent fold increase in integrated OD (IntDen) ± SEM compared with isotype control (set at 1). $*P = 0.0089$, $**P = 0.0008$. Pathogenicity of C9(G0) mAb in μMT mice. (*E*) Day 14 AD, expressed as percentage, in WT, untreated or μMT mice treated i.v. with 250 μg of the indicated mAb. Values represent mean ± SEM; each symbol represents an individual mouse. $*P < 0.01$, $**P < 0.001$, NS, not significant.

without the AP amplification. And lastly, although we have shown here in the mouse model that antibodies activate mainly the LP, it is possible that in humans the autoantigen population directs the autoantibody repertoire and some autoantibodies may activate the CP in addition to the LP, thus explaining the increased expression of C1q. In summary, the results herein support a specific model for the immune response and complement activity in AAA. Further studies are needed to determine its general applicability and to arrive at a balanced approach to any potential complement-based therapeutics aimed at halting disease progression.

Materials and Methods

Animals. WT C57BL/6 and B-cell–deficient (μMT mice, B6.129S2-*Ighm*^{tm1Cgn}/J) mice were obtained from The Jackson Laboratory. fB$^{-/-}$ mice (49) were backcrossed to C57BL/6 for 11 generations. MBL-A/C$^{-/-}$ mice (B6.129S4-*Mbl1*^{tm1Kata} *Mbl2*^{tm1Kata}/J, The Jackson Laboratory) on a C57BL/6 background were generously provided by John P. Atkinson (Washington University School of Medicine). All mice were kept in under pathogen-free conditions at Washington University Specialized Research Facility, and all of the experiments were performed in compliance with federal laws and strictly according to protocols approved by the Division of Comparative Medicine at Washington University School of Medicine.

Human Tissues. Human abdominal aorta tissue specimens were obtained from consented patients at time of elective surgery through a protocol approved by the Institutional Review Board (IRB) at Washington University School of Medicine. Sera were obtained from consented individuals through a protocol approved by the IRB at Washington University School of Medicine. The excess human tissues used in these studies were provided anonymously.

In Situ Immunoprecipitation. Six WT C57BL/6 mice were perfused with elastase and their aortas were randomly harvested immediately or 30 min after elastase perfusion following extensive transcardial flushing with PBS (to remove circulating blood). The flushed aortas ($n = 3$ per time point) were pooled and homogenized. Aortic homogenates were cleared by centrifugation and incubated with protein G-Sepharose beads (Sigma) for 60 min at 4°C, precipitated, and washed extensively. The protein G-bound samples were eluted, fractionated on a 10% (wt/vol) SDS/PAGE gel under reducing conditions, and protein bands were visualized by staining with Sypro Ruby. The experiment was repeated with another cohort of mice ($n = 6$ total) and bands that consistently appeared de novo or were enhanced at 30 min were excised and submitted to the Proteomics Core at Washington University for identification by MS.

Generation of Anti-Fibrinogen mAb. Splenocytes and lymphocytes from naïve WT C57BL/6 mice were fused with Sp20 myeloma cells by standard protocol established by the Hybridoma Center at Washington University. Clones were selected by an ELISA-based assay for reactivity against purified mouse fibrinogen (Innovative Research). We screened 1,116 hybridoma clones and found two (G10 and C9) that produced supernatants with reactivity against fibrinogen. Their reactivity to fibrinogen was confirmed with two additional rounds of subcloning and repeat screening. To purify mAbs, the hybridoma cell lines were grown until 95% cell death to produce hybridoma exhausted supernatants. These exhausted supernatants from G10 and C9 hybridomas

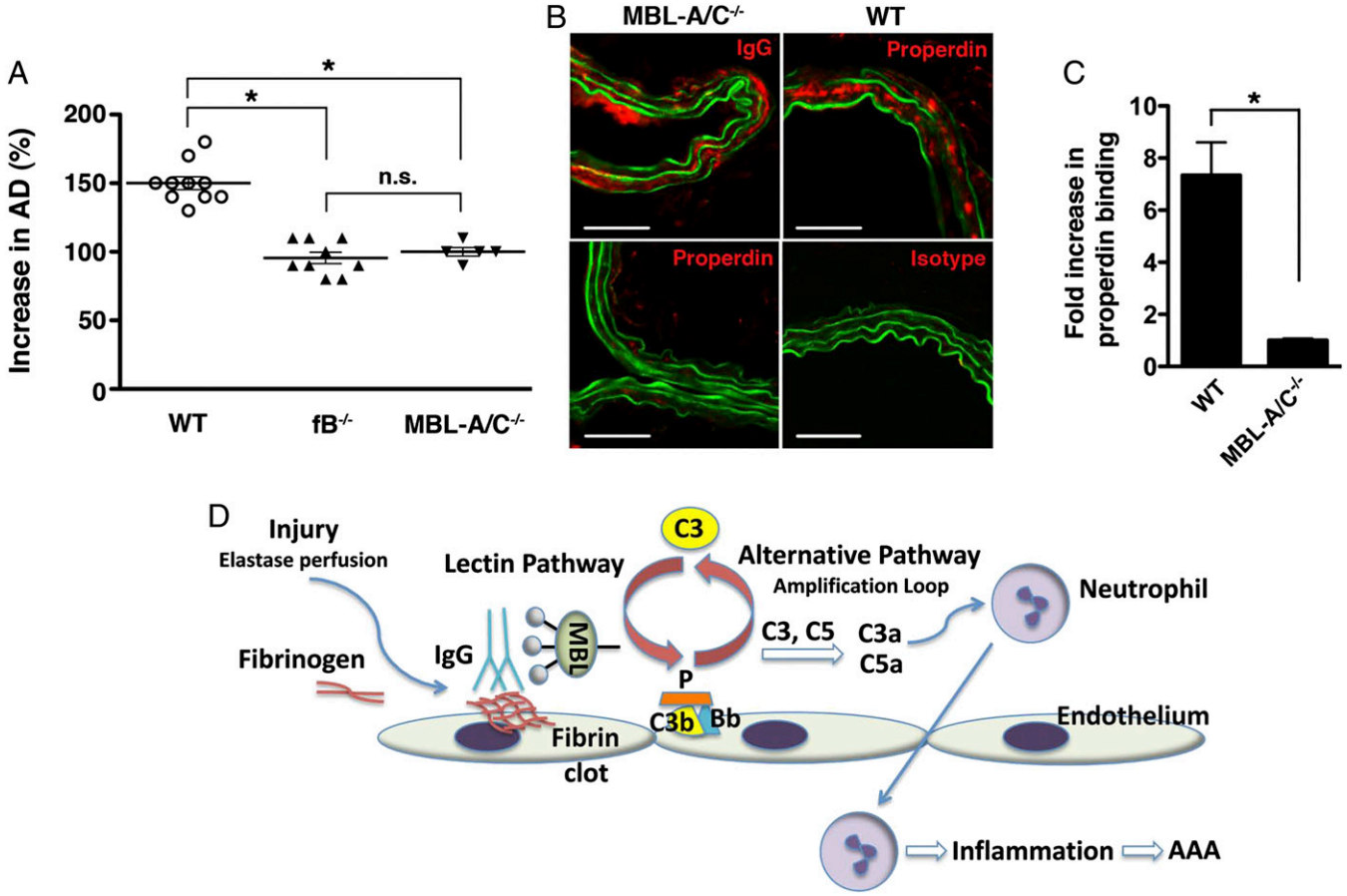

Fig. 6. The LP contribution to elastase-induced AAA. (*A*) Mice were perfused with elastase on day 0 and day 14. AD was measured and expressed as increase in percentage (%). Mice deficient in MBL-A and MBL-C (MBL-A/C$^{-/-}$) were as resistant to elastase-induced AAA as the AP factor B-deficient (fB$^{-/-}$) mice. Each symbol represents an individual mouse. Values represent mean ± SEM *$P < 0.001$; NS, not significant. (*B*) IgG (red) binding to elastase-perfused aorta is independent of MBL-A/C. In contrast, there was minimal properdin (red) deposition in MBL-A/C$^{-/-}$ perfused aorta, whereas properdin was found in abundance in WT perfused aorta. Armenian hamster IgG served as isotype control for anti-properdin mAb (H4). (Scale bar, 50 μM.) (*C*) Quantitative analysis of properdin deposition in abdominal aortas 30 min after elastase perfusion. $n = 3$ aortas per genoytpe, six to nine sections per aorta. Values represent fold increase in integrated OD (IntDen) ± SEM in WT compared with MBL-A/C$^{-/-}$ (set at 1). *$P = 0.0004$. (*D*) Schematic of the order of events in murine elastase-induced AAA. Elastase perfusion triggers local injury, inducing fibrinolysis/fibrin clot formation and revealing neoepitopes that are recognized by natural antibodies. MBL binds antibodies and the immune complex initiates LP activation and properdin-stabilized convertase (C3bBbP) assembly, with subsequent amplification by the AP. Complement activation leads to the generation of anaphylatoxins (C3a, C5a) that attract neutrophils, setting up the inflammatory cascade and culminating in the eventual aneurysmal development.

were purified on a protein-G column, concentrated, and dialyzed extensively against PBS. Isotyping (Southern Biotechnology Associates) revealed that both of G10 and C9 mAbs are IgG2b, κ. F(ab′)$_2$ fragment of G10 mAb was prepared with F(ab′)$_2$ preparation kits (Thermo Fisher Scientific) according to the manufacturer's instructions and verified by SDS/PAGE at every step. To generate IgG(G0), C9 mAb was digested with 40 units/mL of β-galactosidase from *Escherichia coli.* (Sigma) for 72 h at 37 °C, dialyzed extensively against PBS pH 7.4, and concentrated. Concentration of mAb was determined by measuring the *A* at 280 nm of the samples and depletion of terminal galactosylation was confirmed by analysis on SDS/PAGE gel and blotting with ECL.

Elastase-Induced AAA. AAA was induced in 8- to 12-wk-old male mice as previously described (10, 19). Briefly, mice were anesthetized with 55–60 mg/kg i.p. sodium pentobarbital. A laparotomy was performed under sterile conditions. The abdominal aorta was isolated and the preperfused AD was measured with a calibrated ocular grid. Temporary 7-0 silk ligatures were placed around the proximal and distal aorta to interrupt proximal flow. An aortotomy was created at the inferior ligature using the tip of a 30-gauge needle and the aortic lumen was perfused for 5 min at 100 mmHg with a solution containing 0.145 units/mL type 1 porcine pancreatic elastase (Sigma). After removal of the catheter, the aortotomy was repaired without constriction of the lumen to restore the flow. At day 14, a second laparotomy was performed and the perfused segment of the abdominal aorta was reexposed and unblinded quantitative digital readout of AD was obtained in situ by two individual observers before euthanasia and tissue procurement. AD was assessed on day 14 unless otherwise indicated. AAA is defined as an increase in AD of greater than 100% over preperfused diameter. In some experiments, mice were randomly assigned to receive an i.v. injection of 250 μg of the specified purified antibody. For in vivo IgG binding and complement activation studies, the aortas were harvested at 30 min after mAb injection and deposition of IgG/complement proteins was analyzed by immunofluorescence and quantified by ImageJ (see below).

Immunohistochemistry. Immunohistochemistry (IHC) was performed as previously described (10). Briefly mouse abdominal aorta was dissected, snap-frozen in optimal cutting temperature compound, and sectioned at 9 μm. Elastin was stained with Verhoeff-van Gieson (VVG) using an Accustain Elastic Stain kit (Sigma). SMC content was evaluated using an alkaline phosphatase-conjugated antibody to alpha-smooth muscle actin (1:200 dilution; A5691. clone 14A; Sigma). Elastin degradation and SMC actin content were graded on a scale of 1–4 as previously described (11). Grading was performed by an observer blinded to the genotype or treatment. Data presented were derived from nine serial cross-sections that spanned the entire abdominal aorta, $n = 5$ aortas per genotype or treatment.

Cross-sections of human aortic tissues (9 μm) were fixed in 2% paraformaldehyde, blocked in 10% donkey serum (Sigma) in PBS, and incubated with rabbit anti-human MBL antibody (2 μg/mL; sc-25615; Santa Cruz Biotechnology),

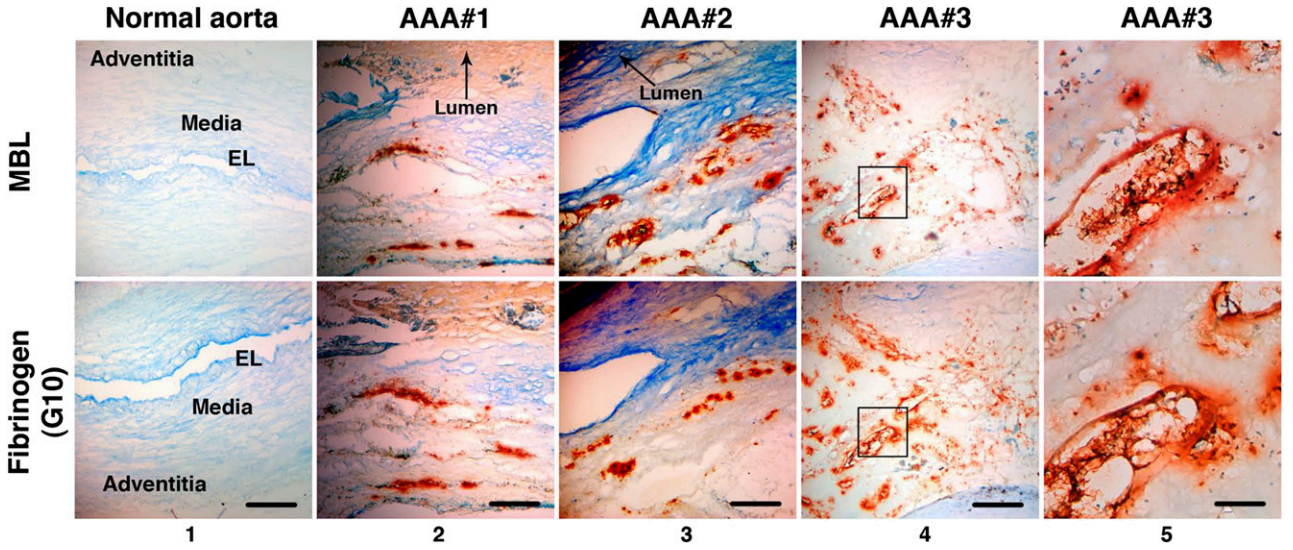

Fig. 7. LP activation in human AAA. Immunohistochemistry performed on serial AAA sections demonstrates that MBL (orange-brown) localized to the same areas as fibrinogen (orange-brown, detected with G10 mAb) in three separate AAA tissue samples. Staining was confirmed on at least three independent sections per tissue sample. Note that the normal aortic wall architecture and layers are distorted in AAA tissues (columns 2–4) due to extensive remodeling and transmural inflammation, as evidenced by inflammatory cell infiltrates and lipid deposition (Fig. S2). Scale bar, 500 μm (columns 1–4); 100 μm (column 5). Panels in column 5 represent higher magnification of *Inset* in column 4. EL, elastic lamellae.

mouse monoclonal anti-human CD68 antibody (1:200 dilution; ab955; Abcam), or G10 mAb (10 μg/mL) for 1 h at room temperature (RT). The sections were washed and incubated with HRP-conjugated anti-rabbit secondary antibody (0.16 μg/mL; 711-035-152; Jackson ImmunoResearch Laboratories) or HRP-conjugated anti-mouse antibody (0.16 μg/mL; 715-035-150; Jackson ImmunoResearch Laboratories). Aortic sections were also incubated with human sera (1:5,000 dilution) washed, then incubated with HRP-conjugated anti-human antibody (0.16 μg/mL; 709-035-149; Jackson ImmunoResearch Laboratories) followed by color development with an HRP substrate kit (Kirkegaard & Perry Laboratories). Aortic sections stained with anti-rabbit secondary antibody (0.16 μg/mL; 711-035-152; Jackson ImmunoResearch Laboratories) or IgG2b, κ-isotype (10 μg/mL; 400393; Biolegend) served as controls for MBL

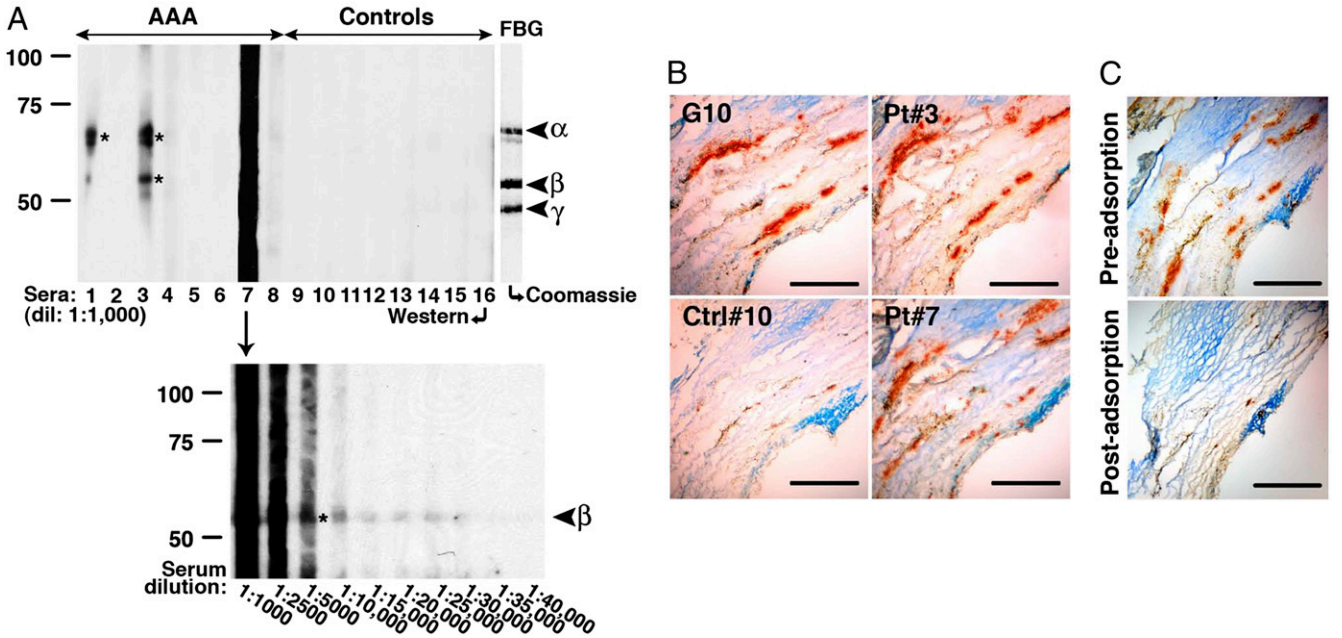

Fig. 8. Detection of circulating antibodies to fibrinogen in individuals with AAA. (*A*) Sera (at the indicated dilution) from AAA patients (Pts), but not controls (Ctrls), recognize different chains of human fibrinogen (asterisks), as determined by Western blot analysis. Coomassie-blue stained gel (*C*, *Right*) indicates the position of fibrinogen α-, β-, and γ-chains. Circulating antibodies from Pt 7 reacted strongly to the β-chain, which was not evident until the serum was diluted to ≥1:5,000. Reactivity to fibrinogen was confirmed on three separate blots. (*B*) Sera from Pt 3 and Pt 7 (1:5,000 dilution) reacted at sites in AAA tissues that correspond to sites of fibrinogen deposition, as detected with G10 mAb. Control serum (Ctrl 10) showed low level of reactivity in aneurysmal tissues, which suggests the presence of endogenous IgG detected with the anti-human IgG secondary antibody. (*C*) Specificity of circulating antibodies for fibrinogen was confirmed by preadsorbing AAA sera (Pt 3 and Pt 7) against human fibrinogen (5 μg/mL) before immunohistochemistry (also Fig. S3). Staining pattern was confirmed on at least three independent sections per tissue sample. (Scale bar, 100 μm.)

and G10 specificities, respectively (Fig. S3). In some instances, human sera were preadsorbed against plate-bound human fibrinogen (5 μg/mL) before performing immunohistochemistry as above. Serum IgG concentrations pre- and postabsorption were semiquantitatively assessed by SDS/PAGE (Fig. S3). All sections were counterstained with 1% methyl green. IHC was performed in serial sections for comparison of staining pattern between MBL, fibrinogen, and macrophages ($CD68^+$). All images were acquired with QCapture software on a Nikon Eclipse microscope.

Immunofluorescence. Frozen cross-sections of mouse abdominal aortic tissues were fixed in acetone, blocked in 8% BSA in PBS, and incubated with G10 mAb (2 μg/mL), rat anti-mouse MBL-C (2 μg/mL; HM 1038, clone 14D2; Hycult Biotech), goat anti-mouse C3 (8 μg/mL; 55463; MP Biomedicals), hamster anti-mouse properdin mAb (6 μg/mL, clone H4 generated in house by D.E.H. and P.B.) (Fig. S4), Armenian hamster IgG isoptype control (6 μg/mL; I-140; Leinco Technologies) or rabbit anti-mouse fibrinogen (10 μg/mL; ab34269; Abcam) for 1 h at RT followed by the appropriate fluorescent-conjugated secondary antibody (Jackson ImmunoResearch Laboratories). All images were visualized on a Nikon Eclipse microscope and acquired at the same exposure with QCapture software.

Quantitative Analysis of Immunofluorescence Intensity. All images were visualized on a Nikon Eclipse fluorescence microscope and acquired with QCapture software using the same exposure time. Single-color images were loaded into the ImageJ program (http://rsb.info.nih.gov/ij) for analysis. A region of interest (ROI) was drawn around the whole aorta with the free-hand selection tool to include the intima and media but excluding non-specific staining in the adventitia. Threshold was adjusted to highlight the intensity of the areas to be analyzed according to negative and positive staining controls. All images were set to the same hue, saturation, and brightness. The area and fluorescence intensity (integrated density) in the ROI were then measured and analyzed. Data were obtained from three to four nonoverlapping fields per aortic cross-section, six to nine sections per aorta (n = 3 aortas per treatment or genotype). Images were loaded into ImageJ and analyzed in a blinded fashion. Results are presented as mean integrated OD (IntDen) or fold increase over control, which was set at 1.

Western Blot Analysis. Purified mouse collagen types I and III (2 μg; AbD Serotec) and mouse fibrinogen (2 μg; Innovative Research) were fractionated on an 8% SDS/PAGE gel under reducing conditions and stained with Coomassie or blotted with C9 or G10 mAb (2 μg/mL) followed by HRP-conjugated anti-mouse IgG (0.16 μg/mL; 715-035-150; Jackson ImmunoResearch Laboratories). Monoclonal antibodies, untreated or treated with β-galactosidase, were also blotted with biotinylated *E. cristagalli* lectin (5 μg/mL; Vector Laboratories) followed by ExtrAvidin-HRP (2 μg/mL; E2886; Sigma). Bands were visualized using a SuperSignal Western Blotting kit (Thermo Fisher Scientific).

Purified human fibrinogen fractionated on an 8% SDS/PAGE gel was blotted with sera from controls or AAA patients (1:1,000–1:40,000 dilution) followed by HRP-conjugated anti-human IgG (0.16 μg/mL; 709-035-149; Jackson ImmunoResearch Laboratories). Bands were visualized using a SuperSignal Western Blotting kit (Thermo Fisher Scientific).

In Vitro MBL-Binding Assay. ELISA plates were coated overnight with 10 μg/mL of the indicated mAb for 16 h at 4 °C. After blocking with 0.1% human serum albumin, the plates were washed and incubated with 100 μL of serial dilutions of WT or MBL-A/$C^{-/-}$ mouse sera (0.1%, 1%, or 10% vol/vol) overnight at 4 °C. After washes, the plates were incubated with rat anti-mouse MBL-C monoclonal antibody (0.4 μg/mL; HM 1038, clone 14D12; Hycult Biotech) followed by incubation with anti-rat-HRP (0.16 μg/mL; 112-035-167; Jackson ImmunoResearch Laboratories). Color was developed with the addition of 100 μL of 1-StepTM Turbo TMB-ELISA (Thermo Fisher Scientific) and read at 450 nm (SpectraMax Plus; Molecular Devices). Specific MBL binding was calculated by subtracting background reading generated by MBL-A/$C^{-/-}$ serum from reading generated by WT serum. Combined data from three independent experiments of triplicates were analyzed and presented.

Statistics. Comparisons between two groups were performed by two-tailed, unpaired t test without correction. Grading data were analyzed with χ^2 test. Comparisons between multiple groups (≥3) were performed by one-way ANOVA. Equality of variance assumption was tested and Bonferroni's correction for multiple comparisons was performed. Normality assumption appeared to be met and tests for equality variance were conducted. The sample size (number of animals per genotype per treatment) chosen is based on means and variances in similar experiments in this mouse model of AAA for detection of differences of 0.05 between experimental groups with a statistical power of 0.80, assuming a two-sided alpha of <0.05. F test was used to compare variances within each group of data and the difference in variances was found to be not significant between groups.

ACKNOWLEDGMENTS. The authors thank Dr. John Atkinson for critical reading of the manuscript and helpful scientific insights, Dr. Kathleen Sheehan and Misha Hart for guidance in the production of mouse and Armenian hamster hybridoma cell lines, Lynne Mitchell and Marilyn Leung for hybridoma screening and cultivation, Richard Haubart for antibody purification, and Dr. Dirk Spitzer for providing the mouse properdin cDNA clone. This work was supported by National Institutes of Health (NIH) Grants AI049261 and AR056468, a bridge fund from the Department of Medicine at Washington University in St. Louis (to C.T.N.P), and NIH Grant AI051436 (to D.E.H.). Experimental support was also partially provided by the Hybridoma Center and the Protein Production and Purification Facility of the Rheumatic Diseases Core Center (NIH P30AR048335). We also thank the Alvin J. Siteman Cancer Center at Washington University School of Medicine and Barnes-Jewish Hospital in St. Louis for the use of the Proteomics Core, which provided mass spectroscopy service. The Siteman Cancer Center is supported in part by a National Cancer Institute (NCI) Cancer Center Support Grant P30 CA91842.

1. Cosford PA, Leng GC (2007) Screening for abdominal aortic aneurysm. *Cochrane Database Syst Rev* (2):CD002945.
2. Gratama JW, van Leeuwen RB (2010) Abdominal aortic aneurysm: High prevalence in men over 59 years of age with TIA or stroke, a perspective. *Abdom Imaging* 35(1): 95–98.
3. Mell MW, et al. (2012) Predictors of emergency department death for patients presenting with ruptured abdominal aortic aneurysms. *J Vasc Surg* 56(3):651–655.
4. Thompson RW (2002) Detection and management of small aortic aneurysms. *N Engl J Med* 346(19):1484–1486.
5. Ballard DJ, Filardo G, Fowkes G, Powell JT (2008) Surgery for small asymptomatic abdominal aortic aneurysms. *Cochrane Database Syst Rev* (4):CD001835.
6. Koch AE, et al. (1990) Human abdominal aortic aneurysms. Immunophenotypic analysis suggesting an immune-mediated response. *Am J Pathol* 137(5):1199–1213.
7. Bobryshev YV, Lord RS (2001) Vascular-associated lymphoid tissue (VALT) involvement in aortic aneurysm. *Atherosclerosis* 154(1):15–21.
8. Kuivaniemi H, Platsoucas CD, Tilson MD, 3rd (2008) Aortic aneurysms: An immune disease with a strong genetic component. *Circulation* 117(2):242–252.
9. Thompson RW, et al. (2006) Pathophysiology of abdominal aortic aneurysms: Insights from the elastase-induced model in mice with different genetic backgrounds. *Ann N Y Acad Sci* 1085:59–73.
10. Pagano MB, et al. (2009) Complement-dependent neutrophil recruitment is critical for the development of elastase-induced abdominal aortic aneurysm. *Circulation* 119(13): 1805–1813.
11. Zhou HF, et al. (2012) Antibody directs properdin-dependent activation of the complement alternative pathway in a mouse model of abdominal aortic aneurysm. *Proc Natl Acad Sci USA* 109(7):E415–E422.
12. Xia S, Ozsvath K, Hirose H, Tilson MD (1996) Partial amino acid sequence of a novel 40-kDa human aortic protein, with vitronectin-like, fibrinogen-like, and calcium binding domains: aortic aneurysm-associated protein-40 (AAAP-40) [human MAGP-3, proposed]. *Biochem Biophys Res Commun* 219(1):36–39.
13. Hirose H, Ozsvath KJ, Xia S, Gaetz HP, Tilson MD (1998) Immunoreactivity of adventitial matrix fibrils of normal and aneurysmal abdominal aorta with antibodies against vitronectin and fibrinogen. *Pathobiology* 66(1):1–4.
14. Chew DK, Knoetgen J, Xia S, Tilson MD (2003) The role of a putative microfibrillar protein (80 kDa) in abdominal aortic aneurysm disease. *J Surg Res* 114(1):25–29.
15. Ando T, et al. (2013) Autoantigenicity of carbonic anhydrase 1 in patients with abdominal aortic aneurysm, revealed by proteomic surveillance. *Hum Immunol* 74(7): 852–857.
16. Murata K, Motayama T, Kotake C (1986) Collagen types in various layers of the human aorta and their changes with the atherosclerotic process. *Atherosclerosis* 60(3): 251–262.
17. Wolberg AS (2007) Thrombin generation and fibrin clot structure. *Blood Rev* 21(3): 131–142.
18. Standeven KF, et al. (2007) Functional analysis of fibrin gamma-chain cross-linking by activated factor XIII: Determination of a cross-linking pattern that maximizes clot stiffness. *Blood* 110(3):902–907.
19. Pagano MB, et al. (2007) Critical role of dipeptidyl peptidase I in neutrophil recruitment during the development of experimental abdominal aortic aneurysms. *Proc Natl Acad Sci USA* 104(8):2855–2860.
20. Arnold JN, Wormald MR, Sim RB, Rudd PM, Dwek RA (2007) The impact of glycosylation on the biological function and structure of human immunoglobulins. *Annu Rev Immunol* 25:21–50.

21. Jefferis R, et al. (1990) A comparative study of the N-linked oligosaccharide structures of human IgG subclass proteins. *Biochem J* 268(3):529–537.
22. Butler M, et al. (2003) Detailed glycan analysis of serum glycoproteins of patients with congenital disorders of glycosylation indicates the specific defective glycan processing step and provides an insight into pathogenesis. *Glycobiology* 13(9):601–622.
23. Nimmerjahn F, Anthony RM, Ravetch JV (2007) Agalactosylated IgG antibodies depend on cellular Fc receptors for in vivo activity. *Proc Natl Acad Sci USA* 104(20): 8433–8437.
24. Malhotra R, et al. (1995) Glycosylation changes of IgG associated with rheumatoid arthritis can activate complement via the mannose-binding protein. *Nat Med* 1(3): 237–243.
25. Hinterseher I, et al. (2011) Role of complement cascade in abdominal aortic aneurysms. *Arterioscler Thromb Vasc Biol* 31(7):1653–1660.
26. Ando T, et al. (2011) Proteomic analyses of aortic wall in patients with abdominal aortic aneurysm. *J Cardiovasc Surg (Torino)* 52(4):545–555.
27. Lee AJ, Fowkes FG, Lowe GD, Rumley A (1996) Haemostatic factors, atherosclerosis and risk of abdominal aortic aneurysm. *Blood Coagul Fibrinolysis* 7(7):695–701.
28. Takagi H, Manabe H, Kawai N, Goto S, Umemoto T (2009) Plasma fibrinogen and D-dimer concentrations are associated with the presence of abdominal aortic aneurysm: A systematic review and meta-analysis. *Eur J Vasc Endovasc Surg* 38(3):273–277.
29. Sánchez-Pernaute O, et al. (2003) A fibrin based model for rheumatoid synovitis. *Ann Rheum Dis* 62(12):1135–1138.
30. Wegner N, et al. (2010) Autoimmunity to specific citrullinated proteins gives the first clues to the etiology of rheumatoid arthritis. *Immunol Rev* 233(1):34–54.
31. Nose M, Wigzell H (1983) Biological significance of carbohydrate chains on monoclonal antibodies. *Proc Natl Acad Sci USA* 80(21):6632–6636.
32. Jefferis R, Lund J, Pound JD (1998) IgG-Fc-mediated effector functions: Molecular definition of interaction sites for effector ligands and the role of glycosylation. *Immunol Rev* 163:59–76.
33. Rademacher TW, Williams P, Dwek RA (1994) Agalactosyl glycoforms of IgG autoantibodies are pathogenic. *Proc Natl Acad Sci USA* 91(13):6123–6127.
34. van Zeben D, et al. (1994) Early agalactosylation of IgG is associated with a more progressive disease course in patients with rheumatoid arthritis: Results of a follow-up study. *Br J Rheumatol* 33(1):36–43.
35. Takahashi K (2011) Mannose-binding lectin and the balance between immune protection and complication. *Expert Rev Anti Infect Ther* 9(12):1179–1190.
36. La Bonte LR, Dokken B, Davis-Gorman G, Stahl GL, McDonagh PF (2009) The mannose-binding lectin pathway is a significant contributor to reperfusion injury in the type 2 diabetic heart. *Diab Vasc Dis Res* 6(3):172–180.
37. La Bonte LR, et al. (2012) Mannose-binding lectin-associated serine protease-1 is a significant contributor to coagulation in a murine model of occlusive thrombosis. *J Immunol* 188(2):885–891.
38. Schwaeble WJ, et al. (2011) Targeting of mannan-binding lectin-associated serine protease-2 confers protection from myocardial and gastrointestinal ischemia/reperfusion injury. *Proc Natl Acad Sci USA* 108(18):7523–7528.
39. Pavlov VI, et al. (2012) Endogenous and natural complement inhibitor attenuates myocardial injury and arterial thrombogenesis. *Circulation* 126(18):2227–2235.
40. Ratnoff WD, Fearon DT, Austen KF (1983) The role of antibody in the activation of the alternative complement pathway. *Springer Semin Immunopathol* 6(4):361–371.
41. Lutz HU, Jelezarova E (2006) Complement amplification revisited. *Mol Immunol* 43(1–2):2–12.
42. Ji H, et al. (2002) Arthritis critically dependent on innate immune system players. *Immunity* 16(2):157–168.
43. Banda NK, et al. (2008) Initiation of the alternative pathway of murine complement by immune complexes is dependent on N-glycans in IgG antibodies. *Arthritis Rheum* 58(10):3081–3089.
44. Takahashi M, et al. (2010) Essential role of mannose-binding lectin-associated serine protease-1 in activation of the complement factor D. *J Exp Med* 207(1):29–37.
45. Iwaki D, et al. (2011) The role of mannose-binding lectin-associated serine protease-3 in activation of the alternative complement pathway. *J Immunol* 187(7):3751–3758.
46. Banda NK, et al. (2011) Mechanisms of mannose-binding lectin-associated serine proteases-1/3 activation of the alternative pathway of complement. *Mol Immunol* 49(1–2):281–289.
47. Mikuls TR, et al. (2011) Associations of disease activity and treatments with mortality in men with rheumatoid arthritis: Results from the VARA registry. *Rheumatology (Oxford)* 50(1):101–109.
48. Lesher AM, Nilsson B, Song WC (2013) Properdin in complement activation and tissue injury. *Mol Immunol* 56(3):191–198.
49. Matsumoto M, et al. (1997) Abrogation of the alternative complement pathway by targeted deletion of murine factor B. *Proc Natl Acad Sci USA* 94(16):8720–8725.